Front. Earth Sci. 2014, 8(4): 582–594
DOI 10.1007/s11707-014-0429-8

RESEARCH ARTICLE

Energy partitioning and environmental influence factors in different vegetation types in the GEWEX Asian Monsoon Experiment

Fengshan LIU[1,2], Fulu TAO (✉)[1], Shenggong LI[1], Shuai ZHANG[1], Dengpan XIAO[1,3], Meng WANG[1,2]

1 Institute of Geographic Sciences and Natural Resources Research, Chinese Academy of Sciences, Beijing 100101, China
2 Graduate University of Chinese Academy of Sciences, Beijing 100049, China
3 Institute of Geographical Sciences, Hebei Academy of Sciences, Shijiazhuang 050011, China

Abstract Environmental influences upon energy balance in areas of different vegetation types (i.e., forest at Kog-Ma in Thailand and at Yakutsk in Russia, grassland at Amdo in Chinese Tibet and at Arvaikheer in Mongolia, and mixed farmland at Tak in Thailand) in the GEWEX Asian Monsoon Experiment were investigated. The sites we investigated are geographically and climatologically different; and consequently had quite large variations in temperature (T), water vapor pressure deficit (VPD), soil moisture (SM), and precipitation (PPT). During May–October, the net radiation flux (R_n) (in $W \cdot m^{-2}$) was 406.21 at Tak, 365.57 at Kog-Ma, 390.97 at Amdo, 316.65 at Arvaikheer, and 287.10 at Yakutsk. During the growing period, the R_n partitioned into latent heat flux ($\lambda E/R_n$) was greater than that partitioned into sensible heat flux (H/R_n) at Tak and at Kog-Ma. In contrast, $\lambda E/R_n$ was lower than H/R_n at Arvaikheer, H/R_n was less than $\lambda E/R_n$ between DOY 149 and DOY 270 at Amdo, and between DOY 165 and DOY 235 at Yakutsk. The R_n partitioned into ground heat flux was generally less than 0.15. The short-wave albedo was 0.12, 0.18, and 0.20 at the forest, mixed land, and grass sites, respectively.

At an hourly scale, energy partitions had no correlation with environmental factors, based on average summer half-hourly values. At a seasonal scale energy partitions were linearly correlated (usually $p < 0.05$) with T, VPD, and SM. The $\lambda E/R_n$ increased with increases in SM, T, and VPD at forest areas. At mixed farmlands, $\lambda E/R_n$ generally had positive correlations with SM, T, and VPD, but was restrained at extremely high values of VPD and T. At grasslands, $\lambda E/R_n$ was enhanced with increases of SM and T, but was decreased with VPD.

Received August 6, 2013; accepted December 2, 2013

E-mail: taofl@igsnrr.ac.cn

Keywords energy balance, vegetation type, net radiation, latent heat flux, sensible heat flux, short-wave albedo, GEWEX Asian Monsoon Experiment

1 Introduction

As the driving force of the earth's climate system (Eugster et al., 2000), radiation and energy balance are greatly influenced by vegetation (Baldocchi and Vogel, 1996; Pielke et al., 1998). The low albedo and complex vertical structure of forests, compared with natural grasslands, allow forests to absorb more net radiation (Baldocchi et al., 2004; Hammerle et al., 2008). Yet for the same kind of vegetation types, there are different conclusions. The dominant heat partition was to latent heat during the rainy season over the eastern Tibetan prairie, which reversed to sensible heat over the western prairie (Choi et al., 2004). Latent heat was dominant at the steppe of central Mongolia under the conditions of a wet and fully developed canopy (Li et al., 2006). Kosugi et al. (2007) reported that temperate forests had larger consumption of sensible heat than of latent heat even in summers; but other study results showed that more available energy was consumed as latent heat than as sensible heat in summer (Hiyama et al., 2005; Wu et al., 2007). Different results were obtained from cross-site investigations. By comparing five forest types, Matsumoto et al. (2008) found that evapotranspiration of temperate forests in summer (July–August) was larger than that of boreal forests; and that the differences in energy-consumption characteristics were greater between locations than between vegetation types. However, other researchers (e.g., Baldocchi et al., 2000; Barr et al., 2001) showed that forest types had greater influences on energy partitioning than locations.

The reasons for these differences may be due to regional air conditions, e.g., temperature, humidity, water vapor pressure deficit, and wind speed; properties of the objects of study (Kariyeva et al., 2012), e.g., root depth, stomatal conductance, and leaf area index; and soil properties, e.g., soil water content, soil organic content, and soil texture. Boreal forests, which, compared with broad-leaved aspen stands, have low root hydraulic conductivity and stomatal conductance, sparse leaf area index, low precipitation and temperature, had lower evaporation (Baldocchi et al., 2000). Five different forest types located in 53.6°–55.6°N, 98.4°–106.2°W, had different evaporative fractions, which were influenced by the surface conductance to water vapor under the regulation of vapor pressure deficit and soil water content (Barr et al., 2001). The reasons for dissimilar evapotranspiration in another five forests (35.2°–62.2°N, 129.6°–142.3°E) were land-surface characteristics rather than atmospheric evaporation demand (Matsumoto et al., 2008).

No clear understanding had been achieved of how the energy exchange between the atmosphere and ecosystem responds to environmental factors (e.g., Li et al., 2006; Xue et al., 2011). Vegetation transformation (e.g., Yao et al., 2011; Meiyappan and Jain, 2012) may cause different results. Three vegetation types (i.e., forest at Kog-Ma and Yakutsk, grassland at Amdo and Arvaikheer, and mixed farmland at Tak), which are located in different climates in the GEWEX (Global Energy and Water Cycle Experiment) Asian Monsoon Experiment, were chosen as study areas. The objectives of this study are to: 1) understand the common and special environmental influences in energy balance and partitioning for different vegetation types and locations; 2) provide insights into general response functions for modeling energy balance and partitioning processes for regional climate models; and hence to improve land-surface models and future climate change projects.

2 Materials and methods

2.1 Observation sites

We chose five research sites located on the Asian continent (Table 1): two forest sites at Kog-Ma and Yakutsk, two grasslands sites at Amdo and Arvaikheer, and one cultivated farmland site at Tak. The data are part of the GEWEX Asian Monsoon Experiment (GAME) (Sugita et al., 2005), which contains half or one-hourly data of (Table 2) net radiation (R_n), short-wave radiation (R_S), long-wave radiation (R_L), air temperature (T_a), relative humidity (RH), wind velocity (u), wind direction (WD), surface temperature (T_{sf}), ground heat flux (G), sensible heat flux (H), latent heat flux (λE), soil temperature (T_{sl}), soil water content (SM), precipitation (PPT), and pressure (P).

The research sites, which are influenced by the summer monsoon and geographically and climatologically different (Table 1), provide a unique data set to compare energy balance for different vegetation types and locations. Most rain events occurred between May and October, with appropriate temperatures during the growing season at the study areas. All of the sites had at least two years, typically three years or more, of measurements in GAME. For our study, we selected one year with a minimum data gap as the representative (Table 1).

2.1.1 Tak

The Tak site was established in the Chao Phraya river basin about 60 km east from the Tak province, Thailand. The main vegetation in summer was a mixed land cover, consisting of rice paddy, shrubs, and deciduous stands. However, the complexity of land conditions would be considered statistically homogeneous on a regional scale (Toda et al., 2002). Generally, paddy would be seen only during the wet season, and shrub and forest stands during the whole year, with their heights ranging from 5 m to 20 m tall. Meteorological and soil data were measured at around 30 m and –0.1 m, respectively (Table 2, Tak).

2.1.2 Kog-Ma

At Kog-Ma, the vegetation type was evergreen broad-leaved forest located near Chiang Mat, Thailand, at the altitude of 1,300 m. The height of the canopy was approximately 30 m above ground level with a leaf area index (LAI) between 3.5 and 4.5, estimated by a plant canopy analyzer (Li-Cor, LI-2000) (Komatsu et al., 2003, 2005). Meteorological and soil data were obtained from

Table 1 General characteristics of observation sites

Site	Vegetation type	Latitude(N)	Longitude(E)	Altitude/m	Time [b)]
Tak	Mixed land cover [a)]	16°56.38′	99°25.78′	121	1998–2001,1999
Kog-Ma	Hill evergreen forest	18°48.76′	98°54.01′	1,300	1998–2001,1998
Amdo	Grassland	32°14.47′	91°37.51′	4,700	1998–2003,2002
Arvaikheer	Grassland	46°16′	102°47′	1,813	1998–2003,2003
Yakutsk	Larch forest	62°15.30′	129°37.13′	220	1997–2000,1999

a) Rice paddy, shrubs and deciduous tree stands; b) The first item is time span, the second is data typically used in the paper considering continuity.

50.5 m and around –0.1 m, but surface temperature and atmospheric pressure were not measured (Table 2, Kog-Ma).

2.1.3 Amdo

The Amdo site is located in the Tibetan Plateau, which has significant influence on both regional and global scale energy and water cycles because of its high elevation and extensive area (Tanaka et al., 2001; Choi et al., 2004). The dominant vegetation was short-grass prairie at Amdo with the altitude of 4,700 m, which has severe descending effects on air temperature. The short grass was sparse during the dry season. During the monsoon period, LAI increased up to 0.45 with an average grass height of about 0.05 m with grazing (Choi et al., 2004). Meteorological and soil data were collected mostly at 1.55 m and around – 0.1 m, respectively. Soil water content and precipitation data that are important in radiation and energy balances were not available (Table 2, Amdo).

2.1.4 Arvaikheer

The Arvaikheer site was located at the Arvaikheer Airport in the Ongin River Basin. It was covered with grass in summer and thin snow in winter. Since the maximum height of the grass was < 30 cm, components of radiation and energy balance were measured at 1.5 m. Other indexes, including T_a, RH, u, WD, and SM, were measured at several levels, except soil temperature (Table 2, Arvaikheer).

2.1.5 Yakutsk

The Yakutsk site was a larch forest on the left bank of the Lena River. The main species was *Larix gmelinii*, and the stand density was 840 trees/ha. The mean stand height and LAI were 18 m and 1.56, respectively (more details in Ohta et al., 2001, 2008). The measurement height of the components of radiation and energy balance was 32 m. Other indexes, including T_a, RH, u, SM, T_{sl}, were measured at several levels (Table 2, Yakutsk).

2.2 Measurement techniques

The turbulence flux of heat was measured by the Eddy correlation technique (EC), with sampling frequency 10Hz at Tak and Kog-Ma, using the following Eqs. (1) and (2):

$$H = c_p \rho \overline{w't'}, \tag{1}$$

$$\lambda E = L\rho \overline{w'q'}, \tag{2}$$

where ρ means the air density ($kg \cdot m^{-3}$); c_p is the specific heat of air ($J \cdot kg^{-1} \cdot K^{-1}$) at constant pressure; L is the latent heat of vaporization of water ($J \cdot kg^{-1}$); and w', t', q' are the deviation of vertical wind ($m \cdot s^{-1}$), temperature (°C), and specific humidity ($kg \cdot kg^{-1}$, from average values (typically

Table 2 Height (depth for T_{sl}, SM) of environmental observations

	Height/m				
	Tak	Kog-Ma	Amdo	Arvaikheer	Yakutsk
R_n ($W \cdot m^{-2}$)	30	50.5	1.55	1.5	32
R_S ($W \cdot m^{-2}$)	30	50.5	1.55	1.5	32
R_L ($W \cdot m^{-2}$)	30	50.5	1.55	1.5	32
T_a (°C)	35	43.3	YY	YY	YY
RH (%)	35	43.4	YY	YY	YY
u ($m \cdot s^{-1}$)	30	YY	YY	YY	YY
WD (°)	30	50.5	YY	YY	32
T_{sf}(°C)	Y	N	Y	1.5	27.9
G ($W \cdot m^{-2}$)	0.01	0.1	0.1, 0.2	0.03	0.01
H($W \cdot m^{-2}$)	30	50.5	1.55	1.5	32
λE ($W \cdot m^{-2}$)	30	50.5	1.55	1.5	32
T_{sl} (°C)	YY	YY	YY	N	YY
SM (%)	0.05	YY	N	YY	YY
PPT (mm)	Y	0.7	N	0.7	0.7
P (hPa)	1	N	Y	2	1

Y: Includes data without height explanation; N: No data or no available data; YY: At least two heights.
Note: measurement methods are EC at Tak, and Kog-Ma; Bowen Ratio at Amdo, and Yakutsk; Band-pass covariance for latent heat flux, and EC for momentum and sensible heat flux at Arvaikheer. Signal meanings: net radiation (R_n), shortwave radiation (R_S), long-wave radiation (R_L), air temperature (T_a), relative humidity (RH), wind velocity (u), wind direction (WD), surface temperature (T_{sf}), ground heat flow (G), sensible heat flux (H), latent heat flux (λE), soil temperature (T_{sl}), soil water content (SM), precipitation (PPT), pressure (P).

30 minutes). The overbar ($\overline{\ }$) is the time average of w', t', and q' considering discretionary data.

The flux of H and λE were calculated by the Bowen Ratio method (BR) with half-hour time steps at Amdo and Yakutsk using Eqs. (3)–(6) as shown:

$$\beta = H/\lambda E = \gamma \Delta T/\Delta e, \tag{3}$$

$$\lambda E = (R_n - G)/(1+\beta), \tag{4}$$

$$H = \beta(R_n - G)/(1+\beta), \tag{5}$$

$$\gamma = c_p p/0.622L, \tag{6}$$

where β is the Bowen Ratio, and ΔT (°C) and Δe (Pa) are vertical gradient differences of temperature and water vapor, when assuming the same conductance of water and heat that is used in empirical calculations. γ is the psychrometric constant ($Pa \cdot K^{-1}$). At Arvaikheer, H was measured by the EC technique and λE by the BR method.

2.3 Energy balance analysis

We calculated R_n using:

$$R_n = S_d - S_u + L_d - L_u, \tag{7}$$

where S_d and L_d represent downward short-wave and long-wave radiation; S_u and L_u stand for upward short-wave and long-wave radiation, respectively. (S_d–S_u) is the short-wave radiation captured by the ecosystem, and their ratio (S_d/S_u), which is largely dependent on the properties of the surface, is used to study the shortwave reflection coefficient. (L_d–L_u) determine the long-wave radiation the ecosystem obtained, and are influenced by the atmosphere and ecosystem temperature. The R_n the ecosystem achieved is partitioned into three components: λE, H, and G:

$$R_n = \lambda E + H + G. \tag{8}$$

Equation (8) ignores the energy storage term used for heating plant body and canopy-air. G was directly measured by soil heat plates, which were placed at 0.01 m, 0.1 m, 0.1 m, 0.03 m, and 0.01 m in Tak, Kog-Ma, Amdo, Arvaikheer, and Yakutsk site, respectively (Table 2), without considering heat storage above the soil layer.

Data quality check without gap filling was done by the GAME panels. We selected data located in time between 6:30 and 18:30, and $S_d > 200\ W \cdot m^{-2}$ (Yakutsk$>100\ W \cdot m^{-2}$) in order to minimize the effect of low solar angles (Monteith and Unsworth, 1990; Li et al., 2006). We did not fill the data gaps caused by issues such as malfunctioning, precipitation events, sensor maintenance, infrared gas analyzer calibration, or power failure. Average values of daily or monthly R_n, λE, H, and G were calculated to represent their diurnal and seasonal change characteristics, i.e., we believe the residual data can represent the whole situation of fluxes, which may add inaccuracy to the overall performance of the EC system. Baldocchi et al. (2004) filled data gaps using the mean diurnal value method, which was similar to the method used in this study. The energy balance closure calculated using those data were: Tak ($(R_n - G) = 0.9319(\lambda E + H) + 37.83$, $R^2 = 0.6446$), and Kog-Ma ($(R_n - G) = 0.8626(\lambda E + H) - 6.5395$, $R^2 = 0.827$). The reasons for closure failure have been analyzed in detail elsewhere (e.g., Wilson et al., 2002; Heusinkveld et al., 2004; Barr et al., 2006; Foken, 2008); the data gaps in this paper may be an additional cause to consider.

3 Results and discussion

3.1 Meteorological conditions

Meteorological conditions, including VPD, T_a, SM, and PPT at each field site, are characterized in Figs. 1–3. There were two different change trends for VPD (Fig. 1) at research sites. At low latitudes (Tak, Kog-Ma), the VPD had quite different characteristics compared with middle and high latitudes (Amdo, Arvaikheer, Yakutsk). The maximum VPD values emerged in the dry season (November–April) at low latitude and in wet season (May–October) at middle and high latitude. The average VPD values (hPa) in the dry and wet seasons were 16.7 and

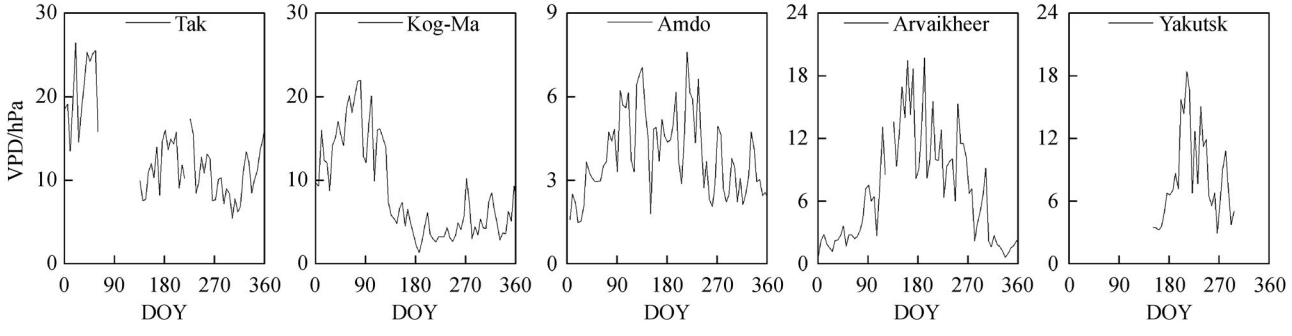

Fig. 1 Seasonal change pattern of water vapor pressure deficit. Data from all sites for $S_d > 200\ W \cdot m^{-2}$ (Yakutsk$>100\ W \cdot m^{-2}$) were used.

10.8 at Tak, 12.1 and 5.1 at Kog-Ma, 3.3 and 4.4 at Amdo, 3.1 and 10.7 at Arvaikheer, and 3.3 and 8.2 at Yakutsk. The average VPD values were 35.3% or 57.9% higher in the dry season than in the wet season at Tak and Kog-Ma, but 25.3%, 71.3%, 59.4% lower at Amdo, Arvaikheer, and Yakutsk, respectively.

Two different variation tendencies for T_a (Fig. 2) were observed at the research sites. There were no apparent seasonal changes at Tak and Kog-Ma. Temperatures at those two places remained at around 27.8°C and 21.5°C throughout the year. At other sites, distinct seasonal patterns were revealed. Temperatures were lower and always below 0°C in winter, higher in spring and autumn, and highest in summer. With latitude increasing, the temperature and above-zero time spans decreased. The temperature at Amdo is significantly influenced by altitude (4,700 m) and the mean was unusually low. Temperatures at Kog-Ma and Arvaikheer were also reduced by elevation.

As shown in Fig. 3, at Kog-Ma and Yakutsk, rainfall frequency (98 vs. 56 times) and amount (1170.7 vs. 256.5

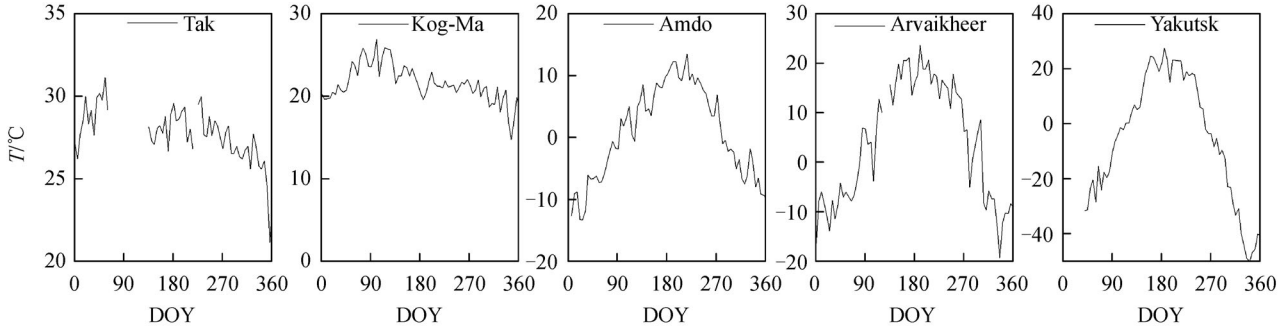

Fig. 2 Seasonal change pattern of atmospheric temperature. Data from all sites for S_d>200 W·m^{-2} (Yakutsk>100 W·m^{-2}) were used.

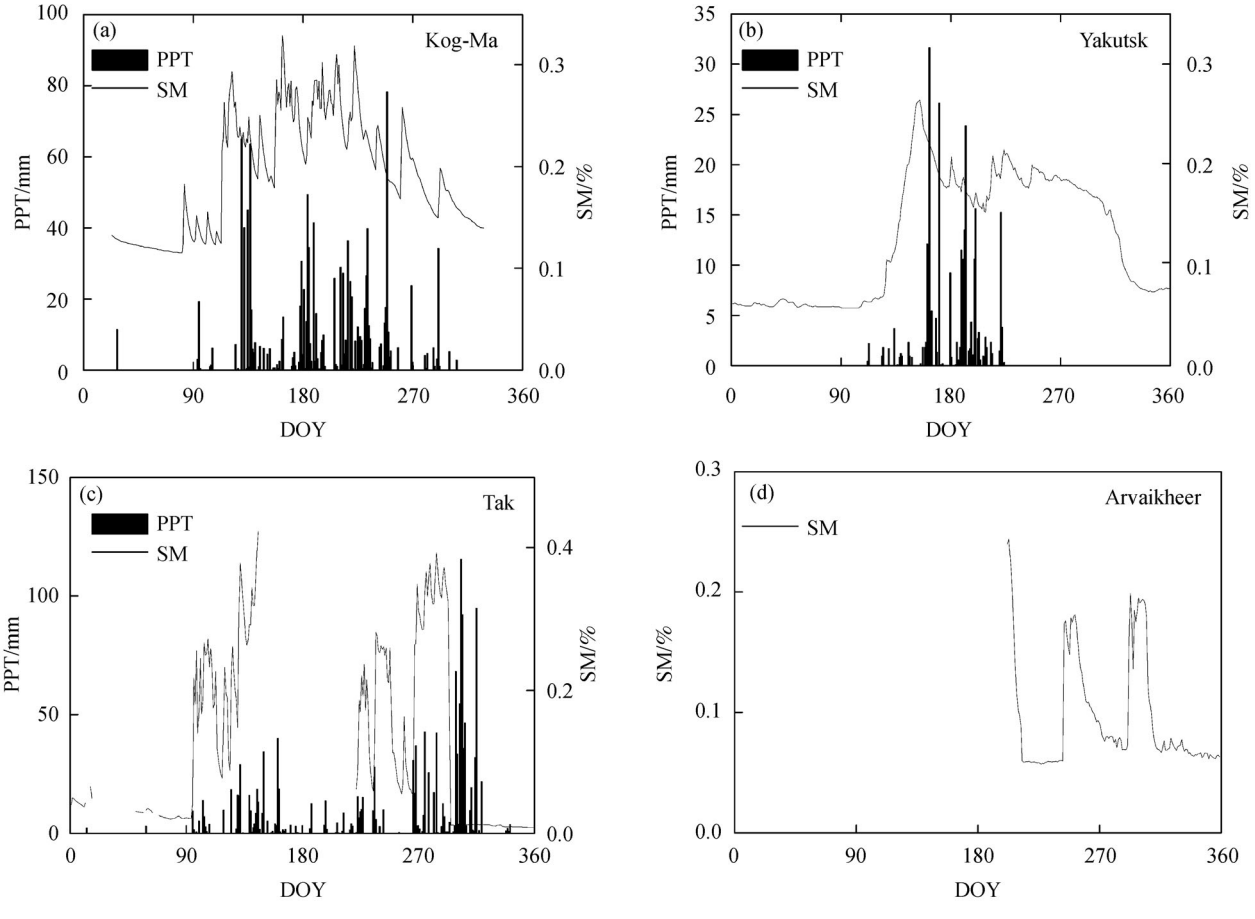

Fig. 3 Seasonal change of soil water content, precipitation and their relationship.

mm) during the wet season were generally higher at Kog-Ma than those at Yakutsk. Soil moisture (0.23 vs. 0.18 $m^3 \cdot m^{-3}$) was higher at Kog-Ma than at Yakutsk due to more water received. The change in soil moisture was related to rain events and evapotranspiration. During the growing season of May–October, the moisture fluctuated smoothly between 0.16 and 0.26 at Yakutsk, but unevenly between 0.16 and 0.32 at Kog-Ma. Between days 250 and 300, soil moisture changed little because of a lack of rain events at Yakutsk. A similar relationship between precipitation and soil moisture existed at Tak site. Owing to the gap of SM at Tak, and lack of precipitation data at Arvaikheer, we didn't analyze its variation rule. But the existing data was used in the study of the environmental controls of energy balance.

3.2 Energy balance

As the energy source of ecosystems, net radiation undoubtedly warrants focus. As shown in Fig. 4, the R_n of average diurnal values for $S_d > 200 W \cdot m^{-2}$ (Yakutsk$>100 W \cdot m^{-2}$) indicated similar change spectrums at the sites, especially in summer. Average diurnal R_n fluctuated between 100 and 600 $W \cdot m^{-2}$ during the growing season (May–October). It fluctuated within the same ranges (200–500 $W \cdot m^{-2}$) in summer. In summer, the average R_n was 406.21, 365.57, 390.97, 316.65, and 287.10 $W \cdot m^{-2}$ at Tak, Kog-Ma, Amdo, Arvaikheer, and Yakutsk, respectively. The Yakutsk site had relatively low R_n values because we defined the time span between 6:30 to 18:30, which abated the advantage of the longer duration of sunshine at high latitudes. In five forest types (35°–62°N, 129°–137°E) (Matsumoto et al., 2008), the daily mean net radiation in summer reached 200 $W \cdot m^{-2}$. Using midday (12:00–16:00 h) values, the R_n of steppe in central Mongolia (47°12′N, 108°44′ E) was 378 $W \cdot m^{-2}$ during May–August (Li et al., 2006). The results of our study differed from those of other investigations due to the time span involved in the computation of the averages.

With the relatively similar energy input, the partitioning patterns of R_n were quite different between sites, confirming the importance of vegetation to the atmosphere (Baldocchi and Vogel, 1996; Pielke et al., 1998). As shown in Fig. 5, although with different variation ranges, the seasonal variations of the ratios of R_n to λE, H, and G were similar at Tak, Amdo, Arvaikheer, and Yakutsk. The ratio of λE to R_n increased from 0.15–0.3 at the beginning of monsoon, maximized to 0.6–0.8 at DOY of 210, and decreased to 0.15–0.3 at the end of the growing period. The variation of H/R_n was reversed from 0.7–0.85 to 0.2–0.4 and back to 0.7–0.85, except at Tak where the variation of H/R_n was from 0.1 to 0.35 to 0.1. At the Amdo site, the ratio of λE (H) to R_n increased (decreased) from 0.2 (0.8) to 0.8 (0.2) and remained so for 2 months. The maximum values of λE (H) to R_n, fitted by a second-order polynomial equation, were 0.50 (0.23) at Tak, 0.76 (0.17) at Amdo, 0.35 (0.49) at Arvaikheer, and 0.54 (0.39) at Yakutsk. The fitted curves also showed $\lambda E/R_n$ greater than H/R_n at Tak, and $\lambda E/R_n$ less than H/R_n at Arvaikheer in the growing period. H/R_n was greater than $\lambda E/R_n$ before DOY 149 and after DOY 270 at Amdo, and before DOY 165 and after DOY 235 at Yakutsk. The ratio of λE (H) to R_n was constant at 0.6 (0.4) during the entire growing period at Kog-Ma. The ratios of G/R_n were generally lower than 0.15, and were influenced mainly by vegetation development (Hammerle et al., 2008).

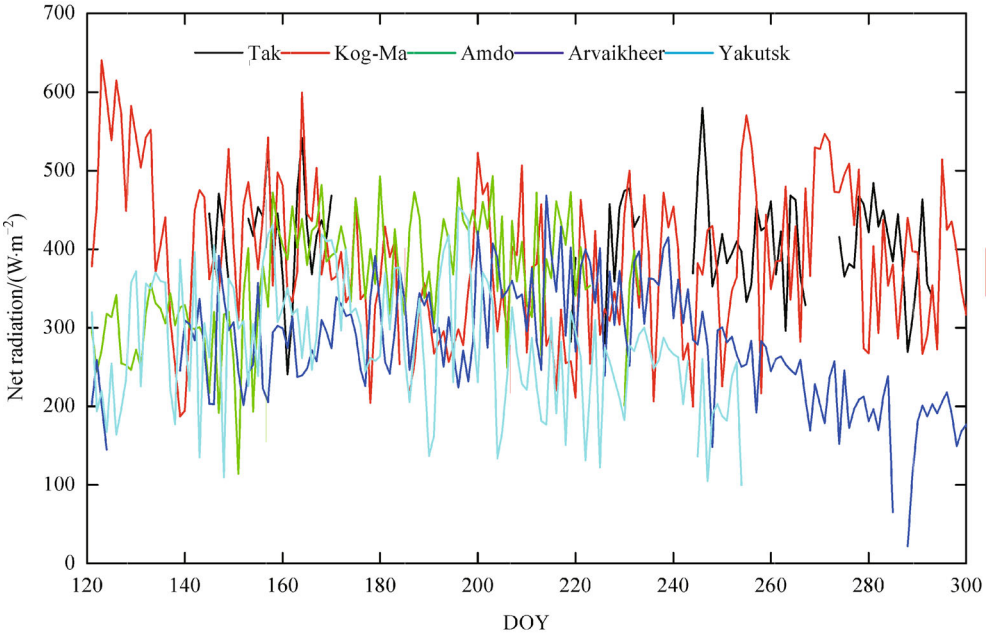

Fig. 4 Seasonal changes of net radiation based on average diurnal values for $S_d > 200 W \cdot m^{-2}$ (Yakutsk$>100 W \cdot m^{-2}$).

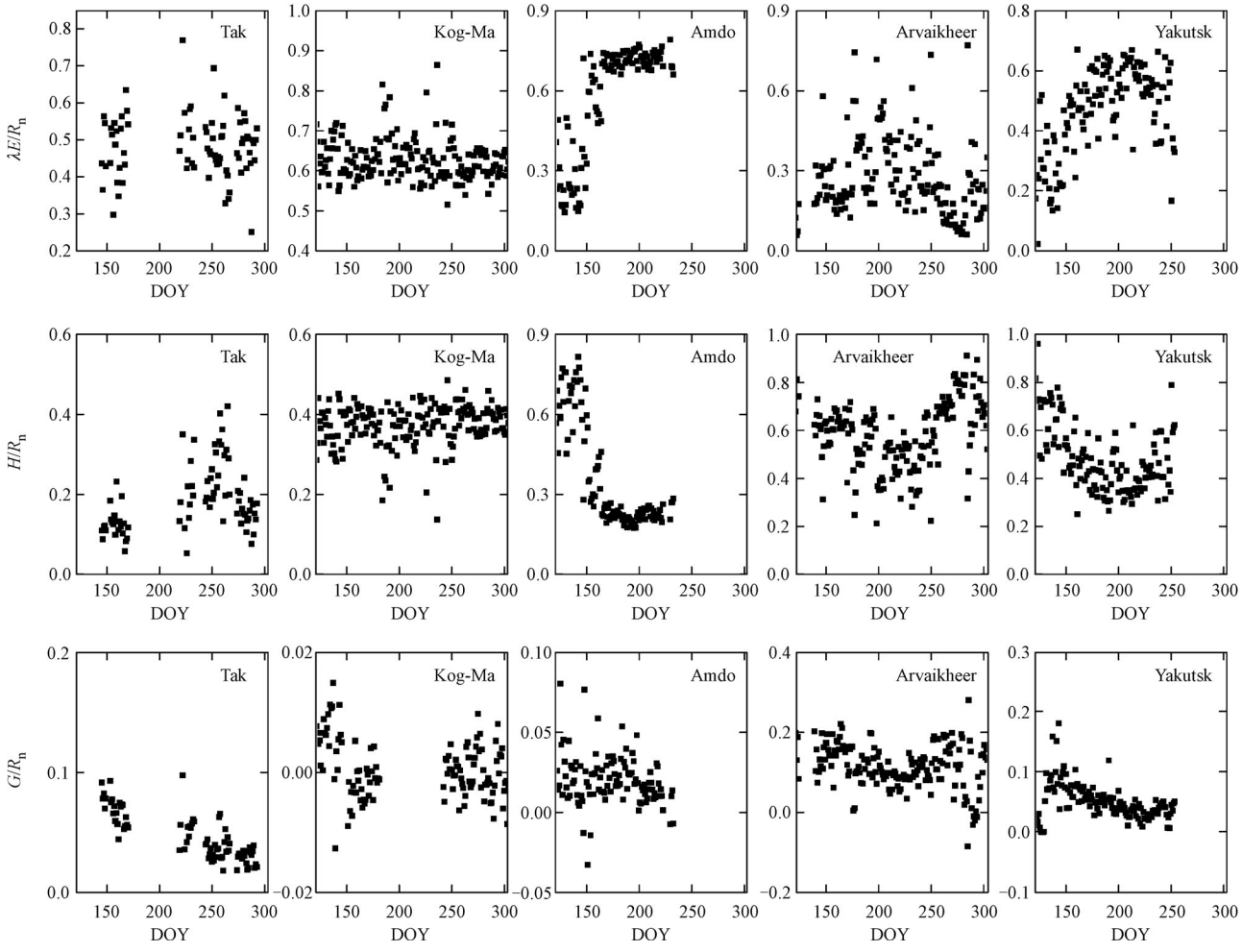

Fig. 5 Seasonal changes of the ratio of R_n to latent heat, sensible heat flux, and ground heat flux (data is average daily value).

The statistical results indicated that energy balance closure was better in summer than in winter (Wilson et al., 2002). The energy balance closure at Tak, which was poor during the early and late growing season, improved in the middle. It was well correlated, but changed little at Kog-Ma. The reasons for a lack of variation of $\lambda E/R_n$ at Kog-Ma may be due to the low VPD (Fig. 1(b)). The forest was often covered by clouds (Masuda, 2004) during the monsoon season, and was supplied by steady water flow from deep soil by a deep rooting system (Tanaka et al., 2008). Thus the lower VPD constrained the rise of $\lambda E/R_n$. At Amdo, low VPD (Fig. 1(c)) also indicated sufficient moisture in the air. In fact, there was frequent precipitation after the onset of the monsoon season (Tanaka et al., 2001), which caused the increase of soil moisture and saturation of the atmosphere. Though Amdo and Arvaikheer had the same vegetation type (grassland), less precipitation at Arvaikheer at < 200 mm (Shinoda et al., 2007) compared with 400 mm at Amdo (Xu et al., 2008) cannot meet the evapotranspiration demand. The rainfall amount was only 265.5 mm at Yakutsk, but the rainfall events occurred mainly between DOY 170 and DOY 250 (Fig. 3), coinciding with the turning point of energy balance (i.e., between DOY 165 and DOY 235 $\lambda E/R_n > H/R_n$).

The partitioning of energy was quite different even for the same vegetation type, necessitating a discussion of external factors, e.g., T, VPD, and SM. First, we addressed the correspondence of the daily change between energy partitioning and environmental factors using averaged summer half-hourly values. Then we investigated seasonal changes of energy partitioning as influenced by ambient conditions using average diurnal values.

3.3 Covariance analysis of energy partitioning and its influence factors

3.3.1 Diurnal scale of energy partitioning and its influence factors

The Kog-Ma and Arvaikheer sites were selected as representative of forest and grassland to provide detailed information on the diurnal course of energy partitioning and environmental factors. As shown in Fig. 6, energy components, partitioning ratios, and influence factors, i.e.,

SM, T, VPD, using average summer half-hourly values, had their own special characteristics as follows.

All of the energy components showed a single peak over time, with a high value at 12:00. The R_n increased from 100 $W \cdot m^{-2}$ in the morning to a peak of 450 $W \cdot m^{-2}$ at 12:00, and decreased to 100 $W \cdot m^{-2}$ in the evening at both sites (Figs. 6(a) and 6(b)). The λE, H, and G had smaller values and variations in magnitude compared with R_n. At

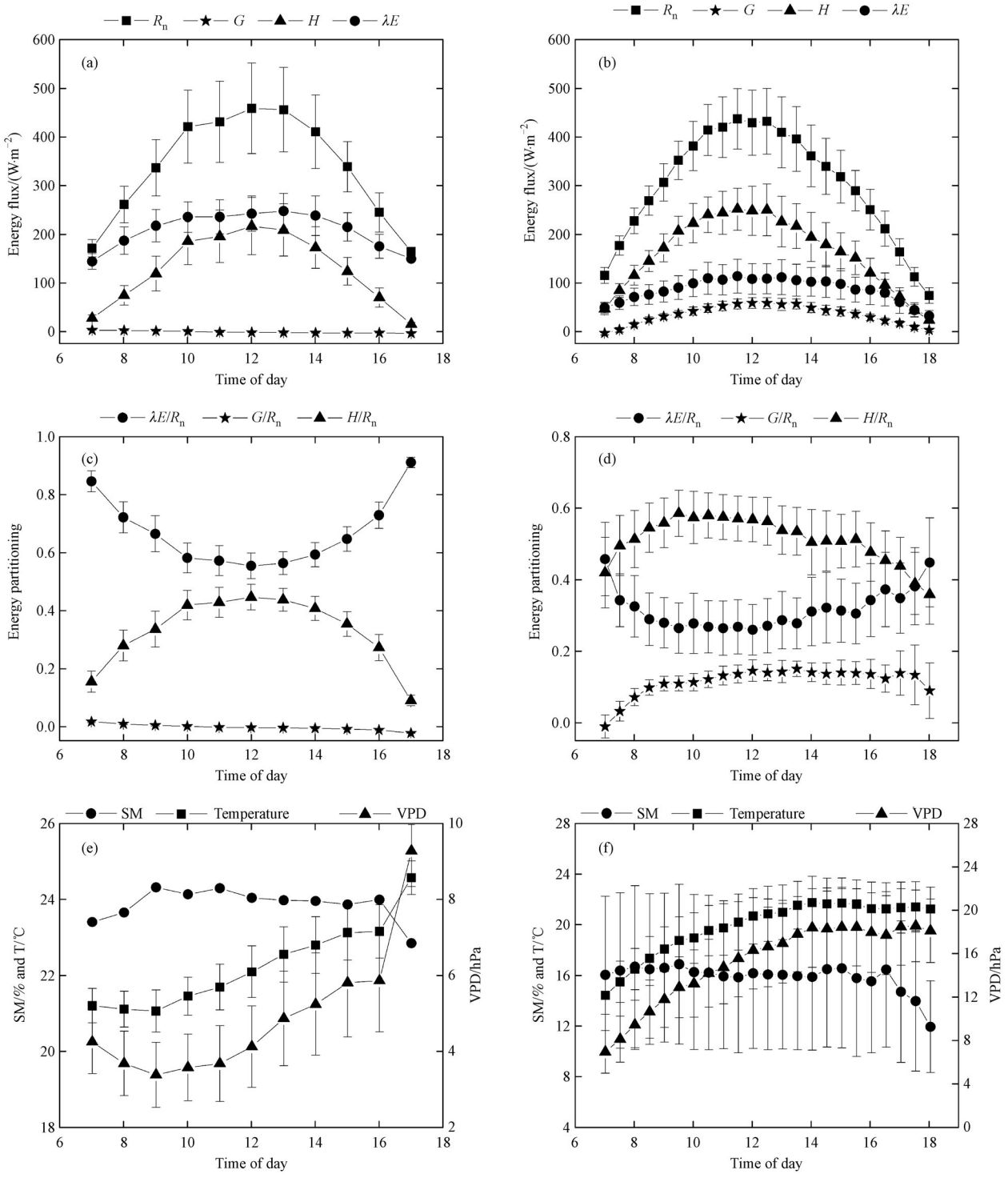

Fig. 6 Daily change of net radiation (R_n), sensible heat (H), latent heat (λE), ground heat fluxes (G); the partitioning fraction of R_n into H, λE and G; soil moisture (SM), temperature (T), water vapor pressure deficit (VPD). Note: two sites were chose to represent the forest and grassland: the left column ((a), (c), (e) was the Kog-Ma site and the right column ((b), (d), and (f) was the Arvaikheer site. The left y axes in (e) and (f) have two units: % for SM, °C for temperature. Bars indicate ±S.E.

the daily scale, $\lambda E/R_n$ had a maximum value in the morning and evening, and a minimum at noon, but the reverse was true for H/R_n at both sites. Net radiation was mostly partitioned to λE (average 400 $W \cdot m^{-2}$) at Kog-Ma and to H (350 $W \cdot m^{-2}$) at Arvaikheer (Figs. 6(a)–(d)). But R_n partitioned more to λE than H in the morning (before 7:00) and evening (later than 17:30) at Arvaikheer. G had a greater value and an increasing ratio to R_n at Arvaikheer than at Kog-Ma because of lower ground coverage (Hammerle et al., 2008). At both sites, T and VPD had similar change patterns, increasing after sunrise, but not stopping even at 17:00. This anomaly coincided with the phenomenon that upward long-wave radiation was always greater than downward long-wave radiation (data not shown). Soil moisture was relatively stable at 24% and 16% at Kog-Ma and Arvaikheer, respectively.

According to Li et al. (2006), daytime H/R_n coincided with horizontal wind speed; bulk canopy surface conductance (g_c) was responsible for the control of λE at water stress conditions; and rain events could significantly increase $\lambda E/R_n$ and g_c as represented by their midday values. The role of stomata on energy partitioning differs under various moisture conditions (Baldocchi et al., 2004). These studies announced the importance of environmental factors. However, in our study, the diurnal change patterns of SM, T, and VPD did not coincide with the characteristics of energy partitioning. Drought is a long event, but energy partitioning is a quick variation process. On a daily basis, soil water cannot change from wet to very dry. But sensible or latent heat can rapidly rise as net radiation increases (Fig. 6, Gu et al., 2006). Even when the soil is very dry, there is still variation of energy components (Crow and Wood, 2002; Gu et al., 2006). Partitioning also differs under various moisture conditions (Fig. 5) as the reaction of g_c and S_d to soil moisture (Li et al., 2006). On a daily basis, energy balance was influenced much by the factors which change rapidly, such as wind speed, net radiation, canopy conductance, thermal stability, and air dryness (Rosset et al., 1997; Burba et al., 1999; Eugster et al., 2000; Li et al., 2006), through stomatal control (Baldocchi et al., 2004).

3.3.2 Seasonal scale of energy partitioning and influence factors

Considering that the diurnal change was investigated using hourly data, the seasonal change of energy partitioning in this sector used average diurnal data (6:30–18:30). This means a larger time scale corresponding to a longer research time scale. Correlation analysis revealed noticeable determination coefficients (usually $p < 0.05$) between SM, VPD, T, and the fraction of R_n to λE at all sites within certain limits, indicating the environmental influences on energy partitioning. The $\lambda E/R_n$ increased to the maximum first, then decreased with the increase of SM and VPD at all sites except Kog-Ma, which exhibited a linear increase. Under the influence of increasing T, $\lambda E/R_n$ showed a rising trend at Amdo, Arvaikheer, and Yakutsk, a downward single peak curve at Tak, and an upward single peak curve at Kog-Ma.

To simplify modeling and energy partitioning limit factors at the Asian Monsoon area, we investigated combined trends for individual vegetation types. The overall variations of $\lambda E/R_n$ were increasing for forest areas (Fig. 7(a)) and grassland (Fig. 7(b)), and were relatively constant for Tak (Fig. 7(c)) with the enhancement of soil moisture. The variations between $\lambda E/R_n$ and temperature (Figs. 7(g), (h), and (i)) were similar for the three vegetation types, but more scattered for grassland. The relevance of $\lambda E/R_n$ to VPD was different, with a positive correlation in forestland and mixed land cover, and a negative correlation in grassland.

The sites used in this study had different seasonal variations in VPD, T_a, SM, and PPT (Figs. 1–3). Especially for the same vegetation types, different meteorological forces caused similar responses in $\lambda E/R_n$. This proved that vegetation has a strong impact on regulation in surface energy partitioning into λE, so as into H. But due to the big difference in meteorological conditions between sites, the causes of diverse answers between vegetation types were unclear relative to vegetation or meteorological conditions. Our results are consistent with previous studies. For example, a study conducted in a typical steppe in Mongolia (Li et al., 2006) demonstrated that water was the limiting factor and $\lambda E/R_n$ was increased (decreased) with enhanced soil water content (VPD). In the Far East, the ET limits of inter-regional forests were land-surface characteristics rather than differing VPD (Matsumoto et al., 2008). The ET of high-latitude ecosystems decreased with declining soil moisture (Eugster et al., 2000). Our study showed a shortage of soil water in the Asian monsoon region, consistent with the results of Tao and Zhang (2011). Under future scenarios of increased soil moisture (e.g., Thomas, 2000; Tao and Zhang, 2011), the partitioning of R_n to λE will increase, and to H will decrease, through which regulate the regional climate response to global warming.

3.4 Short-wave albedo

As the most important factor influencing net radiation, seasonal variations in short-wave albedo are shown in Fig. 8. The forest (Kog-Ma, Yakutsk) had lower albedo, at about 0.12. In the grasslands (Amdo, Arvaikheer) albedo was at 0.2. The average albedo value of Tak was 0.18. The albedo was higher than 0.7 and 0.8 at DOY 150 and DOY 290 at Amdo and Arvaikheer, respectively, caused by temperatures falling below 0°C for one week and covering plants with ice.

The short-wave albedo of the vegetation was related to plant LAI, aboveground dry matter, vegetation structure,

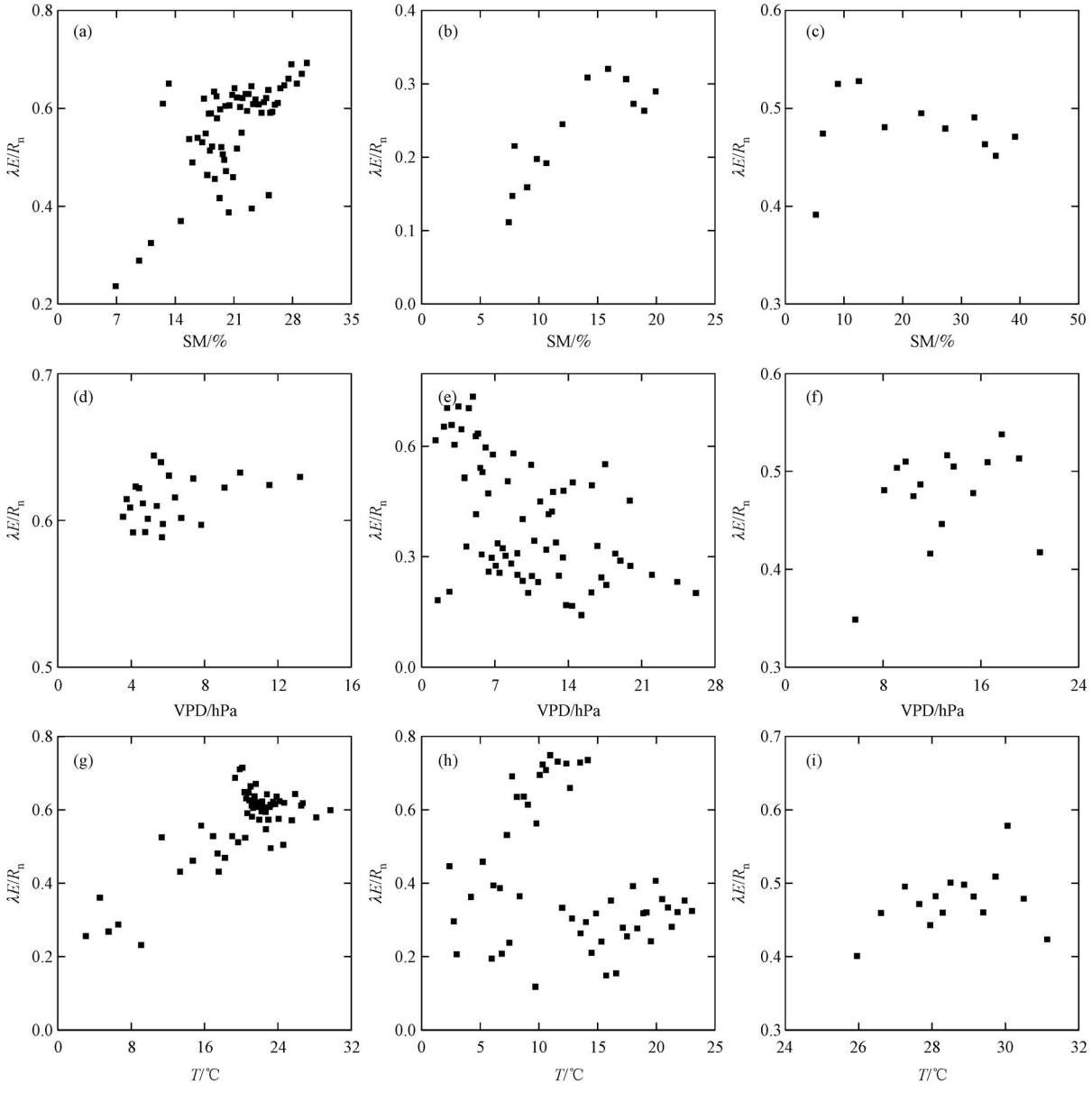

Fig. 7 Seasonal congregated variation trend of all and different vegetation types. Note: (a), (d), (g) for forest at Kog-Ma and Yakutsk; (b), (e), (h) for grassland at Amdo and Arvaikheer; (c), (f), (i) for Tak. Linear regression, (a) $y = 0.014x + 0.275$, $p < 0.001$, $R^2 = 0.4$; (b) $y = 0.061x^2 - 0.0018x + 0.22$, $R^2 = 0.8$, $p < 0.001$; (c) $y = 0.008x^2 - 1.86*10^{-4}x + 0.418$, $R^2 = 0.08$, $p = 0.29$; (d) $y = 0.0023x + 0.6$, $R^2 = 0.09$, $p = 0.0895$; (e) $y = -0.0142x + 0.542$, $R^2 = 0.23$, $p < 0.001$; (f) $y = 0.0426x^2 - 0.0014x + 0.189$, $R^2 = 0.30$, $p = 0.045$; (g) $y = 0.0154x + 0.255$, $R^2 = 0.61$, $p < 0.001$; (h) $y = -0.0076x + 0.506$, $R^2 = 0.032$, $p = 0.111$; (i) $y = 0.5x^2 - 0.0086x - 6.79$, $R^2 = 0.25$, $p = 0.07$.

and environmental factors, e.g., SM, snow, wind speed, cloud, solar elevation (e.g., Rosset et al., 1997; Eugster et al., 2000; Baldocchi et al., 2004; Hammerle et al., 2008). An important question is to what extent are observed differences in energy partitioning and surface energy fluxes due to differences in measurement conditions rather than ecosystem properties (Eugster et al., 2000). As for shortwave albedo, two types of grasslands (or forests) located in geographical locations with different climates and plant species shared a similar magnitude of values. Typically, the albedo has a noon-minimum, two-sides-larger diurnal change pattern with the influence of solar elevation angle. Our data showed reasonable diurnal variation characteristics (Fig. 9). The albedo in tropical forests or plantations is usually < 0.16, compared with the albedo of perennial shrubs at < 0.2, and short grassland at>0.25 (Gash and Shuttleworth, 1991). Our results are consistent with other studies (e.g., Moore, 1976; Eugster et al., 2000).

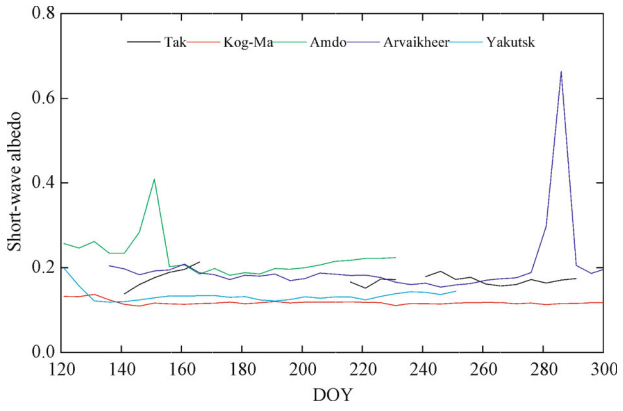

Fig. 8 Seasonal change of short-wave albedo for 5-day average values.

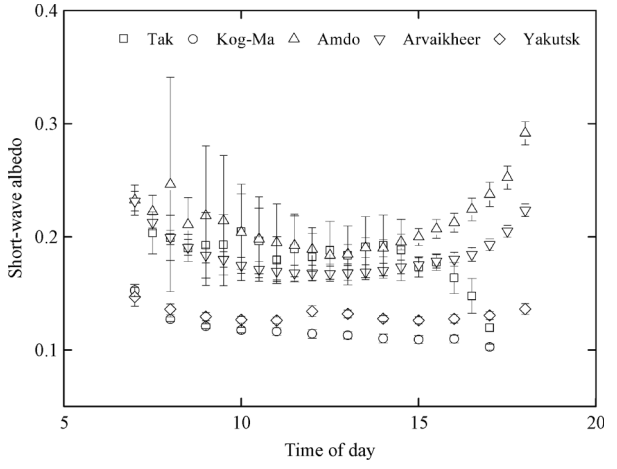

Fig. 9 Diurnal variation of short-wave albedo.

4 Conclusions

Using data from GEWEX Asian Monsoon Experiment, we investigated the energy balance among vegetation types (i.e., forest, grassland, mixed farmland) and their controlling factors in the monsoon zone of Asia. Five sites, which are geographically and climatologically different, provided us with a unique data set to compare energy balance for different vegetation types and climate. Those sites had different variations in temperature, water vapor pressure deficit, soil moisture content, and precipitation.

Different energy balances among vegetation types were presented. In summer (values for $S_d > 200\ W \cdot m^{-2}$, Yakutsk $> 100\ W \cdot m^{-2}$), the average R_n was 406.21 $W \cdot m^{-2}$ at Tak, 365.57 $W \cdot m^{-2}$ at Kog-Ma, 390.97 $W \cdot m^{-2}$ at Amdo, 316.65 $W \cdot m^{-2}$ at Arvaikheer, and 287.10 $W \cdot m^{-2}$ at Yakutsk. Fitted by a second-order polynomial equation, we found that $\lambda E/R_n > H/R_n$ at Tak, $\lambda E/R_n < H/R_n$ at Arvaikheer in the growing period; $H/R_n < \lambda E/R_n$ between DOY 149 and DOY 270 at Amdo, and between DOY 165 and DOY 235 at Yakutsk. The ratio of λE (H) to R_n was constant at 0.6 (0.4) during the entire growing period at Kog-Ma. The ratios of G/R_n were generally lower than 0.15. The albedo was 0.12, 0.18, and 0.20 in the forest, mixed land, and grassland, with greater effects of vegetation than those of climate.

Using average summer half- or one-hourly values, no clear correlations were found between energy partitions and T, VPD, and SM. Using average daily values, there were significant relationships between energy partitions and T, VPD, and SM. The $\lambda E/R_n$ was increased with an increase in SM, T, and VPD at the forest area. At mixed farmland, $\lambda E/R_n$ generally had a positive relationship with SM, T, and VPD, but was restrained at extremely high values of VPD and T. At grasslands, $\lambda E/R_n$ was enhanced with the increase of SM and T, but was decreased with VPD. The lower soil water content can't meet the demand of atmospheric air for water.

Acknowledgements This study was supported by the National Basic Research Program of China (No. 2010CB950902). We greatly appreciate the careful reviews by anonymous reviewers and editors.

References

Baldocchi D D, Kelliher F M, Black T, Jarvis P (2000). Climate and vegetation controls on boreal zone energy exchange. Glob Change Biol, 6(S1): 69–83

Baldocchi D D, Vogel C A (1996). Energy and CO_2 flux densities above and below a temperate broad-leaved forest and a boreal pine forest. Tree Physiol, 16(1–2): 5–16

Baldocchi D D, Xu L, Kiang N (2004). How plant functional-type, weather, seasonal drought, and soil physical properties alter water and energy fluxes of an oak–grass savanna and an annual grassland. Agric Meteorol, 123(1–2): 13–39

Barr A, Morgenstern K, Black T, McCaughey J, Nesic Z (2006). Surface energy balance closure by the eddy-covariance method above three boreal forest stands and implications for the measurement of the CO_2 flux. Agric Meteorol, 140(1–4): 322–337

Barr A G, Betts A K, Black T, McCaughey J, Smith C (2001). Intercomparison of BOREAS northern and southern study area surface fluxes in 1994. J Geophys Res, 106(D24): 33543–33550

Burba G G, Verma S B, Kim J (1999). Surface energy fluxes of Phragmites australis in a prairie wetland. Agric Meteorol, 94(1): 31–51

Choi T, Hong J, Kim J, Lee H, Asanuma J, Ishikawa H, Tsukamoto O, Gao Z, Ma Y, Ueno K (2004). Turbulent exchange of heat, water vapor, and momentum over a Tibetan prairie by eddy covariance and flux variance measurements. J Geophys Res, 109(D21): D21106

Crow W T, Wood E F (2002). The value of coarse-scale soil moisture observations for regional surface energy balance modeling. J Hydrometeorol, 3(4): 467–482

Eugster W, Rouse W R, Pielke R A Sr, Mcfadden J P, Baldocchi D D,

Kittel T G F, Chapin F S III, Liston G E, Vidale P L, Vaganov E, Chambers S (2000). Land-atmosphere energy exchange in arctic tundra and boreal forest: available data and feedbacks to climate. Glob Change Biol, 6(S1): 84–115

Foken T (2008). The energy balance closure problem: an overview. Ecol Appl, 18(6): 1351–1367

Gash J H C, Shuttleworth W J (1991). Tropical deforestation: albedo and the surface-energy balance. Clim Change, 19(1–2): 123–133

Gu L, Meyers T, Pallardy S G, Hanson P J, Yang B, Heuer M, Hosman K P, Riggs J S, Sluss D, Wullschleger S D (2006). Direct and indirect effects of atmospheric conditions and soil moisture on surface energy partitioning revealed by a prolonged drought at a temperate forest site. J Geophys Res, 111(D16): D16102, doi: 10.1029/2006JD007161

Hammerle A, Haslwanter A, Tappeiner U, Cernusca A, Wohlfahrt G (2008). Leaf area controls on energy partitioning of a temperate mountain grassland. Biogeosciences, 5(2): 421–431

Heusinkveld B G, Jacobs A F G, Holtslag A A M, Berkowicz S M (2004). Surface energy balance closure in an arid region: role of soil heat flux. Agric Meteorol, 122(1–2): 21–37

Hiyama T, Kochi K, Kobayashi N, Sirisampan S (2005). Seasonal variation in stomatal conductance and physiological factors observed in a secondary warm-temperate forest. Ecol Res, 20(3): 333–346

Kariyeva J, van Leeuwen W J D, Woodhouse C A (2012). Impacts of climate gradients on the vegetation phenology of major land use types in Central Asia (1981–2008). Frontiers of Earth Science, 6(2): 206–225

Komatsu H, Hotta N, Kuraji K, Suzuki M, Oki T (2005). Classification of vertical wind speed profiles observed above a sloping forest at nighttime using the bulk Richardson number. Boundary-Layer Meteorol, 115(2): 205–221

Komatsu H, Yoshida N, Takizawa H, Kosaka I, Tantasirin C, Suzuki M (2003). Seasonal trend in the occurrence of nocturnal drainage flow on a forested slope under a tropical monsoon climate. Boundary-Layer Meteorol, 106(3): 573–592

Kosugi Y, Takanashi S, Tanaka H, Ohkubo S, Tani M, Yano M, Katayama T (2007). Evapotranspiration over a Japanese cypress forest. I. Eddy covariance fluxes and surface conductance characteristics for 3 years. J Hydrol (Amst), 337(3–4): 269–283

Li S G, Eugster W, Asanuma J, Kotani A, Davaa G, Oyunbaatar D, Sugita M (2006). Energy partitioning and its biophysical controls above a grazing steppe in central Mongolia. Agric Meteorol, 137 (1–2): 89–106

Masuda K (2004). Surface radiation budget: comparison between global satellite-derived products and land-based observations in Asia and Oceania. International Radiation Symposium 2004. Busan, Korea, 2004 (See http://www.jamstec.go.jp/frcgc/research/p2/masuda/radcmp/index.html)

Matsumoto K, Ohta T, Nakai T, Kuwada T, Daikoku K, Iida S, Yabuki H, Kononov A V, van der Molen M K, Kodama Y, Maximov T C, Dolman A J, Hattori S (2008). Energy consumption and evapotranspiration at several boreal and temperate forests in the Far East. Agric Meteorol, 148(12): 1978–1989

Meiyappan P, Jain A K (2012). Three distinct global estimates of historical land-cover change and land-use conversions for over 200 years. Frontiers of Earth Science, 6(2): 122–139

Monteith J L, Unsworth M H (1990). Principles of Environmental Physics (2nd ed). London: Edward Arnold, pp 291

Moore C (1976). A comparative study of radiation balance above forest and grassland. Q J R Meteorol Soc, 102(434): 889–899

Ohta T, Hiyama T, Tanaka H, Kuwada T, Maximov T C, Ohata T, Fukushima Y (2001). Seasonal variation in the energy and water exchanges above and below a larch forest in eastern Siberia. Hydrol Processes, 15(8): 1459–1476

Ohta T, Maximov T C, Dolman A J, Nakai T, van der Molen M K, Kononov A V, Maximov A P, Hiyama T, Iijima Y, Moors E J, Tanaka H, Toba T, Yabuki H (2008). Interannual variation of water balance and summer evapotranspiration in an eastern Siberian larch forest over a 7-year period (1998–2006). Agric Meteorol, 148(12): 1941–1953

Pielke R A Sr, Avissar R, Raupach M, Dolman A J, Zeng X, Denning A S (1998). Interactions between the atmosphere and terrestrial ecosystems: influence on weather and climate. Glob Change Biol, 4(5): 461–475

Rosset M, Riedo M, Grub A, Geissmann M, Fuhrer J (1997). Seasonal variation in radiation and energy balances of permanent pastures at different altitudes. Agric Meteorol, 86(3–4): 245–258

Shinoda M, Ito S, Nachinshonhor G, Erdenetsetseg D (2007). Phenology of Mongolian grasslands and moisture conditions. J Meteorol Soc Jpn, 85(3): 359–367

Sugita M, Nohara D, Miyazaki S, Yamanaka T, Kimura F, Yasunari T (2005). GAME Asian Automatic Weather Station Network (AAN) Data Set Ver.3.0, GAME CD No.13. In: T.E.R.C. GAME AAN Working Group Office, University of Tsukuba, Tsukuba, Ibaraki, Japan

Tanaka K, Ishikawa H, Hayashi T, Tamagawa I, Ma Y (2001). Surface energy budget at Amdo on the Tibetan Plateau using GAME/Tibet IOP98 data. J Meteorol Soc Jpn, 79(1B): 505–517

Tanaka N, Kume T, Yoshifuji N, Tanaka K, Takizawa H, Shiraki K, Tantasirin C, Tangtham N, Suzuki M (2008). A review of evapotranspiration estimates from tropical forests in Thailand and adjacent regions. Agric Meteorol, 148(5): 807–819

Tao F L, Zhang Z (2011). Dynamic response of terrestrial hydrological cycle and plant water stress to climate change in China. J Hydrometeorol, 12(3): 371–393

Thomas A (2000). Climatic changes in yield index and soil water deficit trends in China. Agric Meteorol, 102(2–3): 71–81

Toda M, Nishida K, Ohte N, Tani M, Musiake K (2002). Observations of energy fluxes and evapotranspiration over terrestrial complex land covers in the tropical monsoon environment. J Meteorol Soc Jpn, 80 (3): 465–484

Wilson K, Goldstein A, Falge E, Aubinet M, Baldocchi D, Berbigier P, Bernhofer C, Ceulemans R, Dolman H, Field C, Grelle A, Ibrom A, Law B E, Kowalski A, Meyers T, Moncrieff J, Monson R, Oechel W, Tenhunen J, Valentini R, Verma S (2002). Energy balance closure at FLUXNET sites. Agric Meteorol, 113(1–4): 223–243

Wu J, Guan D, Han S, Shi T, Jin C, Pei T, Yu G (2007). Energy budget above a temperate mixed forest in northeastern China. Hydrol Processes, 21(18): 2425–2434

Xu Z X, Gong T L, Li J Y (2008). Decadal trend of climate in the Tibetan

Plateau—Regional temperature and precipitation. Hydrol Processes, 22(16): 3056–3065

Xue B L, Kumagai T, Iida S, Nakai T, Matsumoto K, Komatsu H, Otsuki K, Ohta T (2011). Influences of canopy structure and physiological traits on flux partitioning between understory and overstory in an eastern Siberian boreal larch forest. Ecol Modell, 222(8): 1479–1490

Yao L, Zhao Y, Gao S J, Li F R (2011). The peatland area change in past 20 years in the Zoige Basin, eastern Tibetan Plateau. Frontiers of Earth Science, 5(3): 271–275